A FEW deg/hr RESOLVABLE LOW NOISE LATERAL MICROGYROSCOPE

Hyung-Taek Lim, Jin-Woo Song, Jang-Gyu Lee and Yong-Kweon Kim

School of Electrical Engineering, Seoul National University,San56-1, Shillim-dong, Gwanak-gu,
Seoul, 151-742, R. O. Korea.
Phone: +82-2-880-1793, Fax: +82-2-873-9953, E-mail: iccari@snu.ac.kr

ABSTRACT

4.68°/hr equivalent noise level microgyroscope is fabricated and tested with a conventional electronic circuits on PCB (Printed Circuit Board). The rate resolution is improved by reduced noise with field coupling compensation and large oscillation amplitude of driven mode.

Unbalanced capacitance variation by fringing field is compensated with mirrored anchor structure. Driven oscillation with enhanced amplitude is mechanically decoupled using folded spring structure, which is independent of the oscillation of sensed mode.

The sensing electronic circuit is realized on PCB using DIP IC, and the capacitance variation in the range of atto-farad is proved through the driven and sensed mode measurement.

Fabricated gyroscope was tested applying 0.01°/sec amplitude with 1 ㎐ sinusoidal input, and showed an equivalent noise level of 4.68°/hr (0.0013°/sec). The microgyroscope is characterized by a linearity error of less than 0.8% FSO for a measured range of ±200°/sec.

INTRODUCTION

Extensive studies on improving performance of microgyroscope have been focused on a symmetric spring design or resonant frequency matching [1-5]. Symmetric structure with matched resonant frequencies enables to amplify its sensitivity by mechanical Q factor of sensed mode. However, actual operation showed mismatched resonance and it was required to balance two resonant modes [1]. In lateral and vertical gyroscopes, as a frequency difference between driven and sensed mode decreases, the mechanical interference increases, and it makes the operation unstable [2-5]. In case of using the same spring for driven and sensed oscillation, a strong mode coupling is shown under resonant frequency difference lower than 100 ㎐ [6].

Mode coupling comes from asymmetries of mass or stiffness and it results in drift and offset of microgyroscopes [1, 4, 7]. In sensing circuit, coupling-like signal is caused by not only mechanical quadrature error [7] but also electric parasitic capacitance that degrades the rate resolution.

In this paper, the restoring spring element for driving and sensing oscillator is independently applied to suppress the coupled oscillation error. The noise by electrostatic field asymmetry is estimated during driven oscillation under no angular rate. A new sensing structure is proposed to balance the sensing capacitance variation by parasitic fields.

Laterally driven and sensing gyroscope is recognized as commercially feasible structure because it needs single mask for definition of gyroscope structure and has the fixed frequencies independent of the structure thickness deviation [7, 8].

In this paper, z-axis microgyroscope with 1×1 ㎟ device size is fabricated with 15 ㎛-thick polysilicon layer, and high aspect ratio electrodes improve sensitivity and reliability to external mechanical perturbation.

PRINCIPLES AND DESIGN

Electromechanical Design

Design of microgyroscope is limited to the device size that can be realized by structure release. Therefore, it needs relevant allocation of driven and sensed elements with mechanical flexures in restricted area.

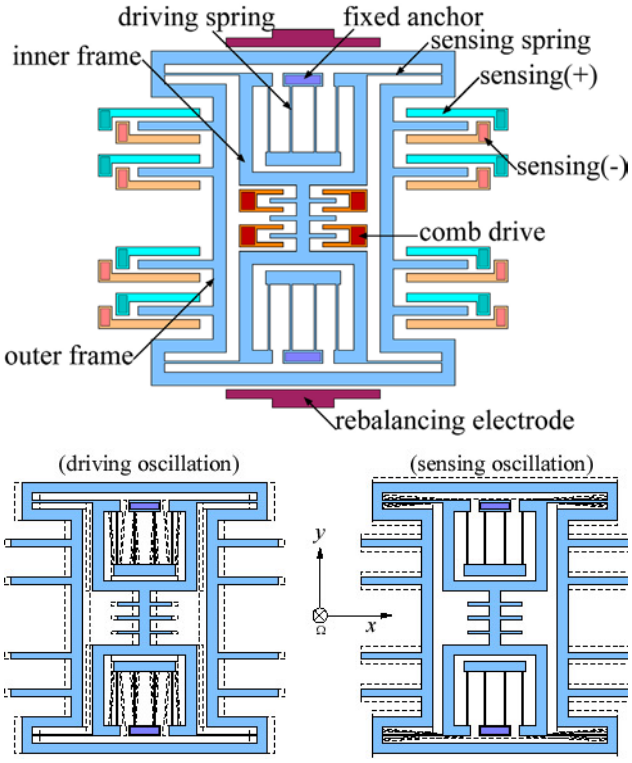

Figure 1. Schematics of decoupled gyroscope

The microgyroscope in this paper is composed of inner driving electrodes, outer sensing electrodes and mass as shown in figure 1. It decreases a parasitic capacitance between electrical interconnection and the larger sensed electrodes area rather than the driven.

The driving and sensing oscillator use independent spring elements to suppress the coupled oscillation. The driven mode flexure is compliant to the driven mode and constraint to its axial direction (sensed mode), and the

sensed is in the same manner. The amplitude of driven oscillation is designed to 40 ㎛ using folded flexure.

Mechanical sensitivity consideration

Vibratory microgyroscope fundamentally operates under the conversion of momentum between two resonators by applied angular rate. It is commonly required to match two frequencies to achieve high sensitivity. However, a smaller difference between two resonant modes raises the more mode coupling and degrades the noise floor and offset.

There are a few operation schemes that raise the mechanical sensitivity of vibratory gyroscope:

(1) Increase of Q factor at low vacuum pressure.

(2) Exact matching of resonant frequencies.

(3) Large amplitude of driven oscillation.

Notice that low vacuum pressure operation at narrow resonant peak would be unstable on slight changes of the resonant frequencies by stiffness hardening, and the applied driven and sensed voltage. Exact matching makes the operation more sensitive to the square of Q and degrades the bias drift.

The amplitude of driving oscillation directly dominates mechanical sensitivity of microgyroscope independent of quality factor and resonance matching. Large amplitude improves sensitivity without any unstable operation.

As shown in Eq. 1, the oscillation and the magnitude of Coriolis acceleration can be expressed as a function of oscillating amplitude and frequency.

$$\begin{aligned} x(t) &= X_0 \sin \omega_x t \\ |\ddot{y}_{Coriolis}| &= 2\Omega_z X_0 \omega_x \\ \frac{|y_{Coriolis}|}{\Omega_z} &= 2Q_y \frac{X_0}{\omega_x} \end{aligned} \tag{1}$$

As a point of reference, for a gyroscope with an oscillation amplitude, X_0=20um, oscillation frequency, ω_x=3KHz, and an applied angular rate,Ω_z=1deg/sec, the mechanical sensitivity of Coriolis deflection is $2.12Q_y$ [*nm*/deg/sec]. Small spring stiffness is required for larger amplitude and smaller resonant frequency in order to increase a mechanical sensitivity.

Electrostatic field coupling error

Suppose that the proof mass mechanically oscillates exactly along driven axis that is perpendicular to the sensed axis, and travels closely to the anchor of sensed electrodes, as shown in figure 2, where no angular rate is applied.

The fringing field between the proof and the anchor of sensing electrode generates the parasitic capacitance. The parasitic capacitance varies with the driving oscillation frequency, and shows an even or odd harmonics at the sensing electronics. The increase and decrease of parasitic capacitance is expressed by Eq. 2 where α and β is defined as geometrical fringing capacitance coefficient. They result in coupled electrostatic force in sensing axis.

$$\begin{aligned} C_{+parastic} &= \alpha|x| \\ C_{-parastic} &= \beta|x| \\ f_{y,parastic} &\propto (\alpha-\beta)|x| \end{aligned} \tag{2}$$

Field compensation

Field-balanced electrode structure is introduced to cancel the force induced by the fringing field. Field-balancing geometrically compensates the partial local field in dense anchor structures by mirroring the anchor position upside down and sideways, as shown in figure 2. There need not any electrical control technique. The net variation of sensing capacitance is cancelled out, as given by Eq. 3.

$$\begin{aligned} f_{y,parastic,upper} &\propto (\alpha-\beta)|x| \\ f_{y,parastic,lower} &\propto (\beta-\alpha)|x| \\ f_{y,parastic,total} &= 0 \end{aligned} \tag{3}$$

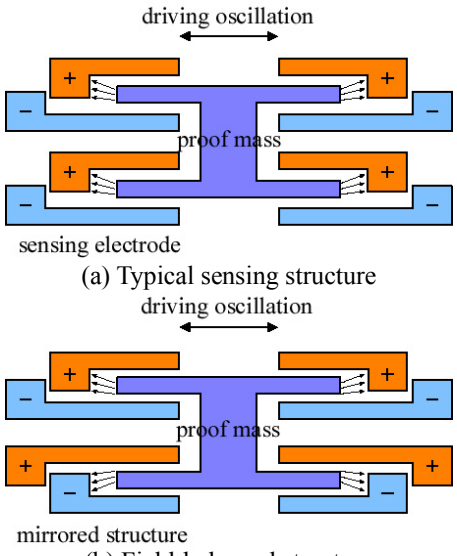

(a) Typical sensing structure

(b) Field-balanced structure

Figure 2. Oblique driving oscillation and balanced motion at no angular rate input.

ANALYSIS

Electrostatic field analysis

Estimation of sensing capacitance and effect of parasitic field was carried out with FEA (ANSYS) analysis. Figure 3 shows the cross-sectional result of distorted electrostatic potential contour by parasitic field in electrode structure. There are sensing electrodes(upper and lower) and proof mass electrode(center) with 2 ㎛ gap and 8 ㎛ separation from anchor. Parasitic capacitance difference by fringing effect is observed within the extent of about 8 ㎛ between anchor and electrode of the proof.

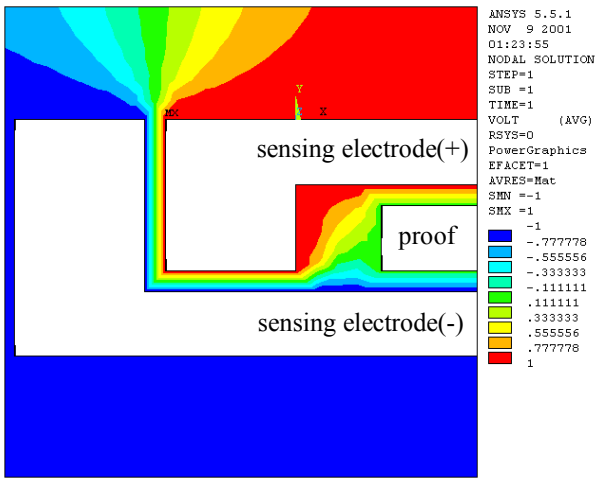

Figure 3. FEA (ANSYS) electrostatic field analysis.

Mechanical analysis

The mechanical design on modal characteristics is verified using FEA analysis (ABAQUS). There are no coupled deflections when the static load is applied to the each resonator in normal direction of oscillation axis. As shown in figure 4, and the driving and the sensing resonant frequency are 3.537 ㎑ and 3.844 ㎑, respectively. The driving frequency separated by 9% from the sensing frequency considering electrostatic frequency tuning.

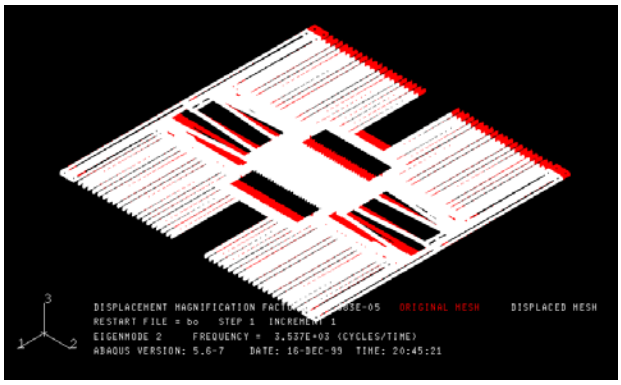

(a) Driving mode-3.537 ㎑

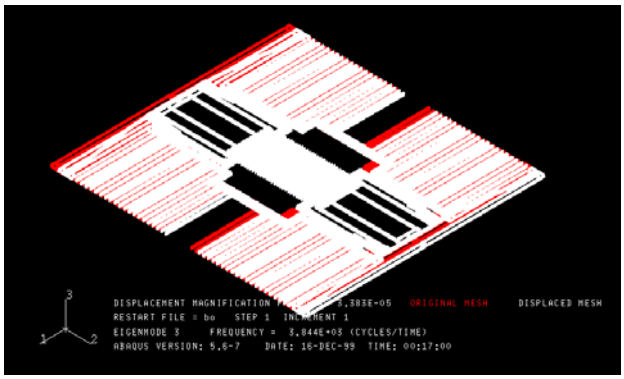

(b) Sensing mode-3.844 ㎑

Figure 4. FEM (ABAQUS) modal analysis

FABRICATION

The microgyroscope is fabricated using a conventional 2-layer polysilicon micromachining with 15 ㎛ thickness in 1×1 ㎟ area. The final microgyroscope is protected by anodic bonding with a preprocessed glass cap with a cavity and feed-through hole for wire bonding, as shown in figure 5.

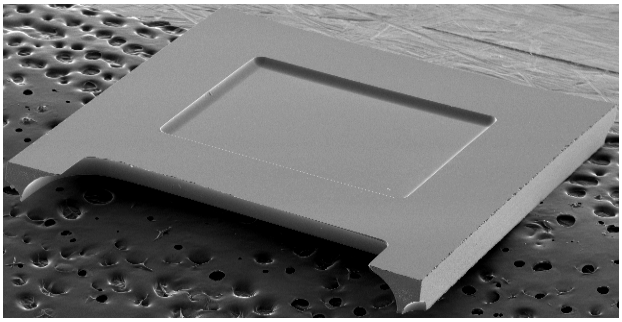

(a) Glass cap (bottom)

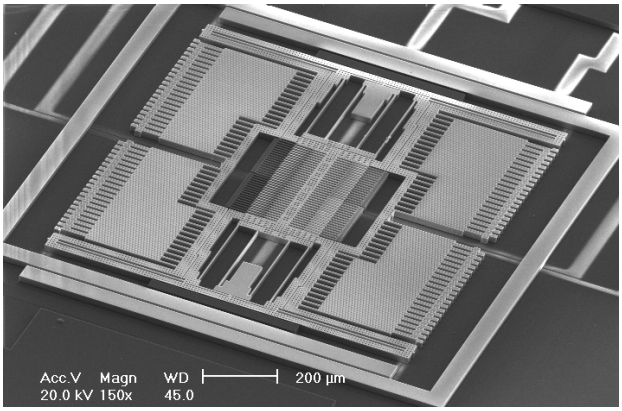

(b) Gyroscope structure

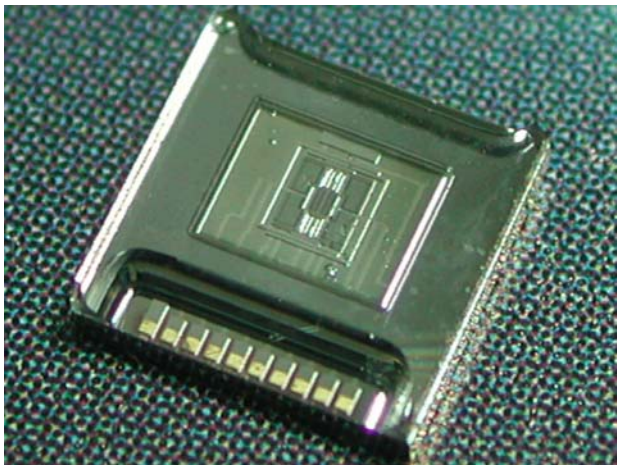

(c) Chip with protective glass cap

Figure 5. Fabricated microgyroscope

TEST AND MEASUREMENT

Resonant mode measurement

Frequency response of the driving and sensing resonant mode is measured by detecting capacitance of comb driving and sensing electrodes, respectively. Figure 6 shows bode plot of driven mode with resonant frequency at 3.08 ㎑. The capacitance of comb driving electrodes is about 70 femto-farad.

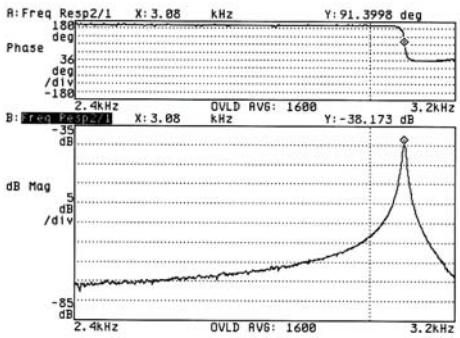

Figure 6. Driving mode frequency response

Capacitance resolution is measured under driving comb electrode into 0.2 ㎛, which is equivalently 0.7 femto-farad capacitance variation, as shown in figure 7.

Compared to S/N ratio, the resolvable capacitance is 4.8 atto-farad.

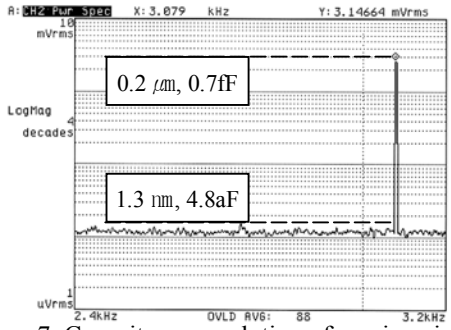

Figure 7. Capacitance resolution of sensing circuit

Rate table test

The fabricated gyroscope with field balanced structure was tested applying 0.01°/sec amplitude with 1 ㎐ sinusoidal input and showed to have a mean noise level of 0.0013°/sec excluding drift below 1 ㎐, as shown in figure 8. The drift below 1 ㎐ region is sourced from PCB, because there is no difference in noise level whether or not the gyroscope package is extracted from PCB.

The measured microgyroscope is characterized by a linearity error of less than 0.8% full scale for a measured range of ±200°/sec as shown in figure 9. The measured bias is stabilized between equivalent rate of less than 0.046°/sec for 1 hour.

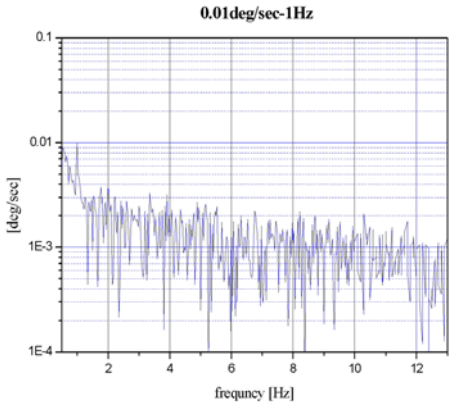

Figure 8. Sensor output at 0.01°/sec, 1 ㎐ rate input

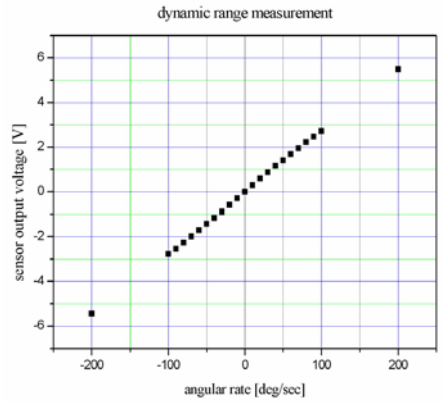

Figure 9. Rate input vs. sensor output

CONCLUSION

A high sensitive and low-noise microgyroscope is designed to comprise a decoupled structure with large driving oscillation amplitude and a field-balanced sensing structure.

The lateral microgyroscope is fabricated in 1×1 ㎟ area using conventional polysilicon micromachining.

The device shows an equivalent noise level of 4.68 deg/hr (0.0013°/sec) and nonlinearity error of 0.8% in ± 200°/sec FSO.

There is room for reducing the measured noise level and bias stability by modification of sensing circuit.

ACKNOWLEDGEMEMTS

Authors are gratefully acknowledging the financial support by ADD (Agency for Defence Development) and by ACRC (Automatic Control Research Center), Seoul National University.

REFERENCES

[1] F. Ayazi and K. Najafi, J. MEMS, "A HARPSS Polysilicon Vibrating Ring Gyroscope", Vol. 10, No. 2. June, 2001, pp.169-179.

[2] S. S. Baek, Y. S. Oh, B. J. Ha, S. D. An, B. H. An, H. Song and C. M. Song, "A Symmetrical Z-axis Gyroscope with a High Aspect Ratio Using Simple and New Process", MEMS'99, pp. 612-617.

[3] H. Kawai, M. Tamura and K. Ohwada, "Direct Measurement of Mechanical Coupling in Microgyroscope Using a Two-Dimensional Laser Displacementmeter", *Transducers'99*, pp. 1566-1569.

[4] Y. Mochida, M. Tamura and K. Ohwada, "A Micromachined Vibrating Rate Gyroscope with Independent Beams for the Drive and Detection Modes",*MEMS'99*, pp. 618-623.

[5] B. L. Lee, Y. S. Oh, K. Y. Park, B. J. Ha, Y. I. Ko, J. G. Kim, S. J. Kang, S. O. Choi and C. M. Song, "A Dynamically Tuned Vibratory Micromechanical Gyroscope-Accelerometer", SPIE, 1997, Vol. 3242, pp. 86-95.

[6] S. An, Y. S. Oh, B. L. Lee and K. Y. Park, "Dual Axis Microgyroscope with Closed-loop Detection", *IEEE/ASME MEMS workshop 99*, pp. 494-499.

[7] A. Clark. R. T. Howe, "Surface Micromachined Z-Axis Vibratory Rate Gyroscope", Solid State Sensor and Actuator Workshop'96, pp. 283-287.

[8] S. H. Kim, J. Y. Lee, C. H. Kim and Y. K. Kim, "A Bulk-micromachined Single Crystal Silicon Gyroscope Operating at Atmospheric Pressure", Transducers'01, pp. 476-479.